

# UC Irvine

## UC Irvine Previously Published Works

### Title

Increased expression of GABA transporters, GAT-1 and GAT-3, in the deafferented superior colliculus of the rat.

### Permalink

<https://escholarship.org/uc/item/3w18k8hc>

### Journal

Brain research, 783(1)

### ISSN

0006-8993

### Authors

Yan, XX  
Ribak, CE

### Publication Date

1998-02-01

### DOI

10.1016/s0006-8993(97)01157-8

### Copyright Information

This work is made available under the terms of a Creative Commons Attribution License, available at <https://creativecommons.org/licenses/by/4.0/>

Peer reviewed

## Research report

# Increased expression of GABA transporters, GAT-1 and GAT-3, in the deafferented superior colliculus of the rat

Xiao-Xin Yan <sup>\*</sup>, Charles E. Ribak*Department of Anatomy and Neurobiology, University of California at Irvine, College of Medicine, Irvine, CA 92697-1275, USA*

Received 16 June 1997; accepted 16 September 1997

---

**Abstract**

GABA transporters (GATs) play a critical role in the transmembrane transport of GABA in neurons and glial cells. Two major brain GATs, GAT-1 and GAT-3, are found in astrocytes in the adult brain. Astroglia demonstrate morphological and molecular changes in response to brain injury and deafferentation. The present study was designed to determine whether the expression of GATs changes after nerve deafferentation using the rat superior colliculus (SC) as a model. The immunoreactivity for GAT-1 and GAT-3, as well as GABA and glutamic acid decarboxylase (GAD)-65 and GAD-67, was studied in the SC of control rats and rats with unilateral optic nerve transections. Immunolabeling for both GAT-1 and GAT-3 was increased in the neuropil of the denervated SC as compared to that for the SC of control rats or for the unaffected SC of experimental rats. In contrast, immunoreactivity for GABA, GAD-65 and GAD-67 was not altered. The change in the immunolabeling of GAT-1 and GAT-3 was detectable at 1 day postlesion and became more evident between 3–30 days postlesion. At the electron microscopic level, immunoreactivity for both GAT-1 and GAT-3 in the unaffected SC was localized to astrocytic processes, whereas GAT-1 immunolabeling was also present in synaptic terminals. In the deafferented SC, immunolabeling for both GATs was elevated in the somata and processes of hypertrophied astrocytes as compared to that in the unaffected SC, whereas GAT-1 labeling in neuronal profiles was largely unchanged. A substantial increase of GAT-1 and GAT-3 in astrocytes following optic nerve transection suggests that these cells play a role in modulating GABA's action in the deafferented SC. © 1998 Elsevier Science B.V.

**Keywords:** GABA transporter; GAD-65; GAD-67; Astrocyte; Enucleation; Neuroplasticity; Neuron-glia interaction

---

**1. Introduction**

The magnitude and duration of GABA's activity are determined by its high affinity transporters that are present on neurons and glial cells [15]. The transport system efficiently clears GABA from the synaptic cleft and surrounding extracellular space following its release [15,41]. There is also evidence that the same system may excrete GABA from neurons and their terminals into the extracellular environment in a  $\text{Ca}^{2+}$ -independent, non-vesicular manner [1,2,17]. Four GABA transporters were cloned and they are classified as GAT-1, GAT-2, GAT-3 and GAT-4 according to their different amino acid sequences and pharmacological properties [4,8,12,19]. Antibodies directed against these proteins and probes for their mRNA were used to study their tissue distribution, and GAT-1 and

GAT-3 have been shown to be brain specific [8,14,32,34,43].

The cellular localization of GAT-1 and GAT-3 was demonstrated in several regions of the adult and developing brain [23,24,32,38,39,43,45]. In the adult rat neocortex and hippocampus, immunolabeling for GAT-1 is localized to axon terminals and astroglia [23,38], whereas that for GAT-3 occurs exclusively in astrocytic processes [24,38]. Furthermore, immunoreactivity for GAT-1 is not found in neuronal somata of the adult at the light microscopic level, but sparse immunolabeling around the Golgi complex in somata is detectable in electron microscopic preparations [38]. More recently, we showed that GAT-1 immunoreactivity is transiently present in the somata and dendrites of neocortical and hippocampal interneurons in developing rats [45]. The subcellular distribution of GAT-1 in these developing interneurons suggested that GAT-1 may be involved in the release of GABA from these neurons, a finding that is consistent with GABA's proposed role as a neurotrophic factor in early stages of cortical development [7,16,49].

---

<sup>\*</sup> Corresponding author. Fax: +1-714-8248549; e-mail: xyan@uci.edu.

Disorganization and/or malfunction of the GABAergic system were found in experimental conditions as well as neurological and psychiatric disorders, such as epilepsy and schizophrenia (e.g., [3,18,29,35–37]). Specifically, recent findings in human epilepsy have shown that the affected temporal lobe displays a reduction in glutamate-stimulated GABA release which indicated a loss of GAT function [10]. Since GATs play an important role in regulating GABA's action, it is of interest to determine whether they are modified in their expression following neuronal injury. In fact, glial cells, particularly astrocytes, display morphological and molecular changes following brain injury, including deafferentation, and some of these changes may affect the function of neurotransmitters, such as glutamate and GABA [28,42,44]. However, the underlying mechanism for this glial regulation of neurotransmission is not well understood. In the present study, the effect of deafferentation on the expression of GAT-1 and GAT-3 was investigated in the rat superior colliculus (SC) after unilateral optic nerve transection. The SC was chosen because it: (1) displays high mRNA signal and strong immunolabeling for both GAT-1 and GAT-3 [8,14,19,24,32], and (2) is particularly suitable for study following deafferentation because the majority of retinal projections to the visual layers of the contralateral SC is affected whereas that to the ipsilateral SC is unaffected [13,20,22,30]. GABA and two isoforms of glutamate decarboxylase, GAD-65 and GAD-67, were also analyzed with immunocytochemical methods in these same preparations. A preliminary report has been presented elsewhere [48].

## 2. Materials and methods

### 2.1. Animals and surgery

Experiments were performed on male and female adult albino rats (Sprague-Dawley) weighing 250–350 g. The experimental animals were anesthetized with sodium pentobarbital (50 mg/kg, i.p.) prior to the surgery for optic nerve transection. Briefly, the right eyeball was separated along its temporal side from other orbital tissue using an operating microscope and microsurgical instruments. After the optic nerve was exposed, it was transected with scissors about 1–2 mm behind the posterior pole of the eyeball. All rats were returned to the vivarium after the surgery and they were allowed to survive for 1 ( $n = 3$ ), 3 ( $n = 4$ ), 7 ( $n = 4$ ), 14 ( $n = 4$ ), 21 ( $n = 3$ ) or 30 ( $n = 4$ ) days. Two additional animals did not undergo this surgery and they served as controls. All of the surgical procedures were approved by the institutional animal research committee at UC Irvine.

### 2.2. Tissue preparation

Control rats and experimental rats at the above-indicated time points were deeply anesthetized with an overdose of sodium pentobarbital and perfused transcardially with 0.12 M phosphate buffered saline (PBS, pH 7.4) followed by 4% paraformaldehyde and 0.5% glutaraldehyde in phosphate buffer (PB, pH 7.4). All brains were removed and postfixed in the perfusion solution for 4–8 h at 4°C, and transferred to cold PBS for several hours to a few days. The midbrain and brainstem were blocked from these brains and the side ipsilateral to the nerve transection was marked. The brain blocks were then sectioned coronally at 30–50  $\mu\text{m}$  with a vibratome, and sections through the SC were collected alternately in tissue-culture wells in PBS and processed for immunocytochemistry.

### 2.3. Immunocytochemistry

Free-floating sections containing the SC were immunostained for GAT-1, GAT-3, GABA, GAD-65 or GAD-67 using the standard avidin–biotin complex (ABC) method. Briefly, endogenous peroxidase activity was bleached with a 20 min rinse in 0.05% hydrogen peroxide ( $\text{H}_2\text{O}_2$ ). Non-specific background staining was blocked by a 2 h incubation in 5% normal horse serum (NHS) at room temperature, after which the sections were incubated overnight at 4°C and with agitation in a PBS solution containing 5% NHS, 0.3% Triton X-100 and one of the following primary antibodies at the indicated dilution. The antibodies directed against GAT-1 and GAT-3 were harvested from immunized rabbits [23,24] and were both diluted at 1:10 000. The mouse GABA antiserum was obtained from Sigma and diluted at 1:20 000. A monoclonal mouse antibody against GAD-65 from Boehringer Mannheim was diluted at 1:2000, whereas the polyclonal rabbit anti-GAD-67 serum from Chemicon was diluted at 1:5000. The specificity of these primary antibodies was tested in previous studies [11,23,24,47]. For a control of the immunostaining, the primary antibody was replaced by PBS or NGS, and section processed in this way displayed no specific immunolabeling. After the incubation with primary antibodies, the sections were further incubated in 1% universal anti-IgG with 5% NHS in PBS for 1 h at room temperature, followed by a 1 h incubation in 1% ABC solution. The immunoreaction product was visualized with 0.05% 3,3'-diaminobenzidine tetrahydrochloride and 0.005%  $\text{H}_2\text{O}_2$ . Three 10 min rinses with PBS were conducted between all incubations. The universal ABC kit was obtained from Vector Laboratories.

### 2.4. Electron microscopy

Electron microscopic preparations were processed for characterizing the ultrastructure of only GAT-1 and GAT-3

immunoreactive profiles because GABAergic neurons and terminals were previously studied in the deafferented SC of rats by electron microscopy using antibodies to GAD and GABA [13,30]. Pre-embedding immunocytochemistry

was used for brain sections from experimental rats that survived for 7 and 14 days. Briefly, 50  $\mu\text{m}$ -thick sections were first immunostained for GAT-1 and GAT-3 as described above, except that Triton X-100 was omitted to

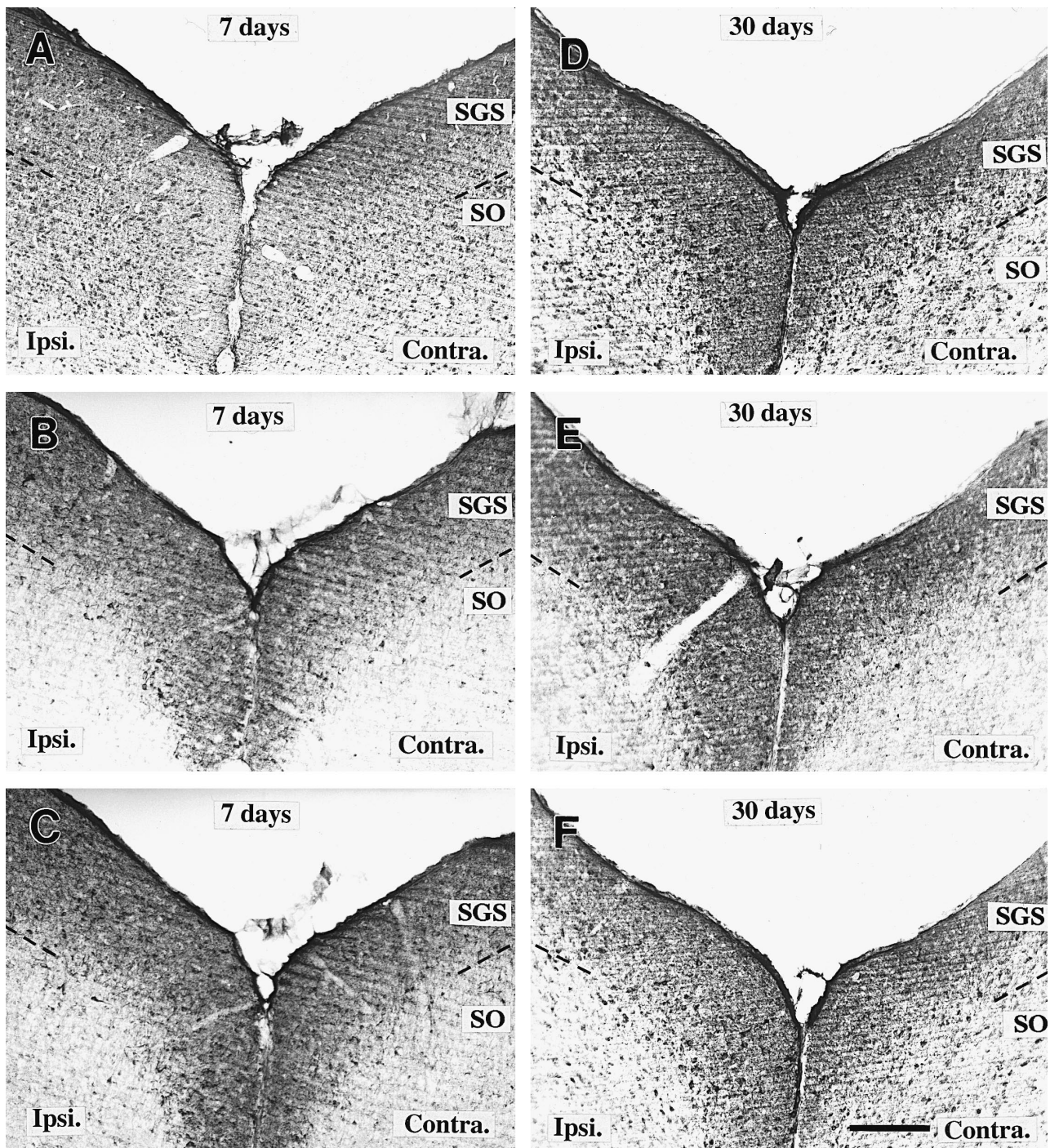


Fig. 1. Photomicrographs of sections through a middle level of the superior colliculus (SC) from rats that survived 7 (A–C) and 30 (D–F) days after unilateral optic nerve transections. The sections were immunostained for GABA (A, D), glutamic acid decarboxylase (GAD)-65 (B, E) and GAD-67 (C, F). GABA immunoreactivity is localized to visual and non-visual layers of the SC, with a denser distribution of labeled somata and neuropil in the stratum griseum superficiale (SGS). GAD-65 and GAD-67 immunolabeled somata and puncta are concentrated in SGS. Note that there is no remarkable difference in the staining intensity and distribution pattern of the immunoreactivities for these GABAergic markers between the contralateral (Contra.) and the ipsilateral (Ipsi.) SC relative to the optic nerve lesion. The superficial layers of the SC are thinner in the contralateral side, and this reduction in thickness is greater at 30 days than at 7 days. SO: Stratum opticum. Broken lines indicate the lower border of the SGS. Scale bar = 100  $\mu\text{m}$ .



preserve the ultrastructure of these sections and the incubation time with primary antibodies was 36–48 h. After immunostaining, selected sections were post-stained with osmium tetroxide, dehydrated with ethanol and acetone, and flat-embedded in Epon. Thin sections were obtained from comparable regions of the ipsi- and contralateral SC, and were stained with uranyl acetate and lead citrate before they were examined with a Philips CM10 transmission electron microscope.

### 3. Results

The distribution of immunolabeling for GABA, GAD and GAT in the SC ipsilateral to the nerve transection from operated animals showed the same laminar pattern as the SC of normal rats. Therefore, the description of the immunoreactivity in the normal rat SC will be from the unaffected SC from operated rats. A comparison of the immunostaining in the SC between the two sides (unaffected and deafferented) of the same operated rats will be

provided following the descriptions of the normal distribution pattern.

#### 3.1. Distribution of GABA and GAD immunoreactivity in the unaffected SC

Light microscopic preparations revealed a greater concentration of GABA and GAD immunostaining in the superficial layers than in the intermediate and deep layers of the SC (Fig. 1). For example, numerous GABA immunoreactive somata were found in the stratum griseum superficiale (SGS), and GABA immunoreactive puncta were densely packed in the stratum zonale (SZ) and SGS. The pattern of immunolabeling for GAD-65 and GAD-67 in the SC was similar to that for GABA immunostaining. However, the number of neuronal somata immunolabeled for GAD appeared less than that for GABA (Fig. 1B–C, E–F). Thus, immunostaining for GAD-65 and GAD-67 was greatest in the SZ and SGS, which contained densely packed puncta and many neuronal somata. The immunoreactive somata for GABA and GADs were mostly small to

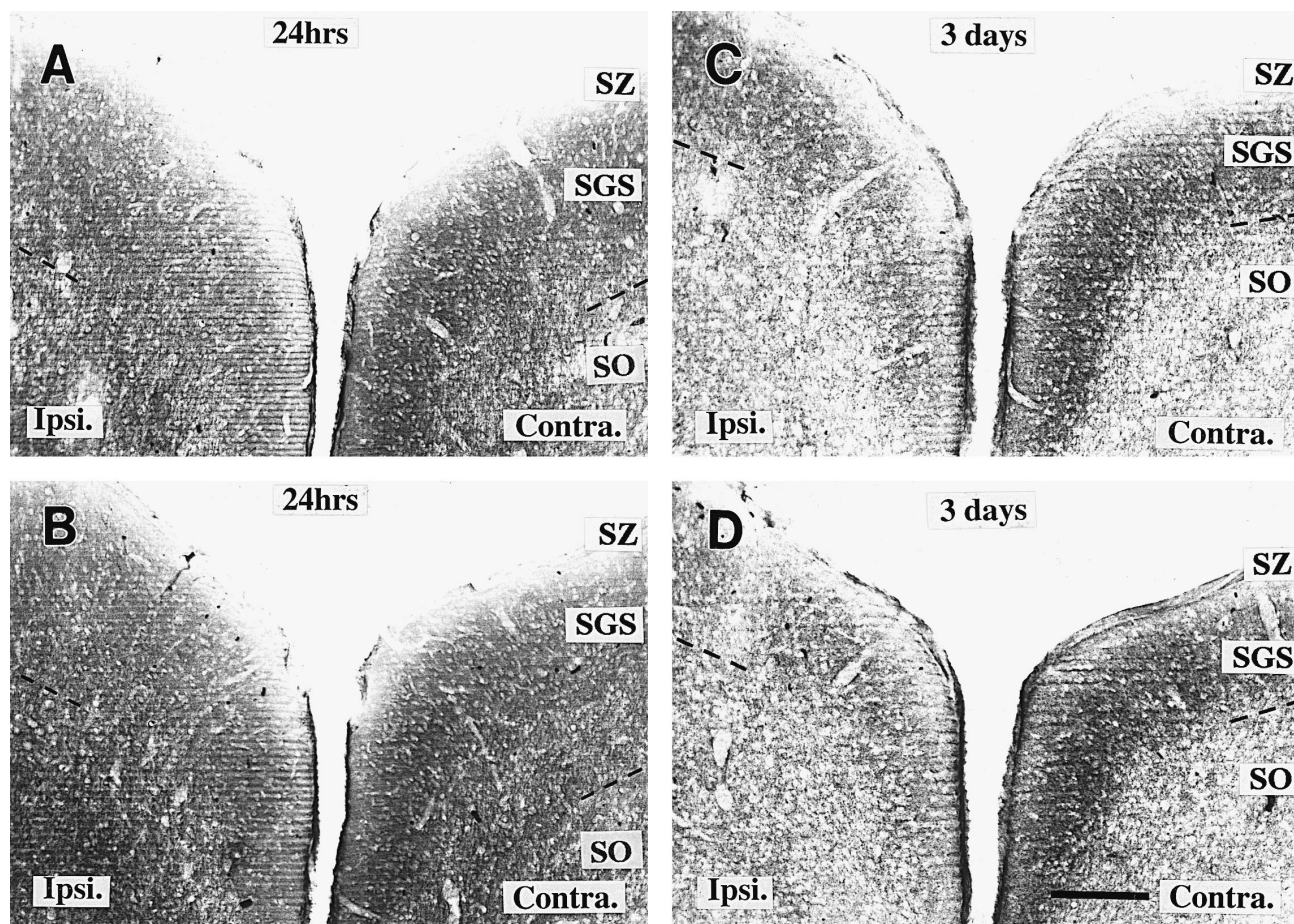


Fig. 2. Photomicrographs showing GAT-1 (A, C) and GAT-3 (B, D) immunolabeling in the SC of rats that survived for 24 h (A, B) and 3 days (C, D) after unilateral optic nerve lesion. The pattern of immunoreactivity in the SC is similar for both GATs. The strongest neuropil labeling is found in the SGS, whereas the stratum zonale (SZ) is lightly immunostained. No immunolabeled somata are present. A slight increase in labeling for GATs is recognizable 24 h after the lesion in the SGS of the contralateral (Contra.) SC (A, B) as compared to the ipsilateral (Ipsi.) SC, and this increase becomes more substantial by 3 days survival (C, D). Broken lines indicate the lower border of the SGS. SO: stratum opticum. Scale bar = 100  $\mu$ m.

medium in size, with only a few large somata that were mainly localized to the border between the SGS and stratum opticum (SO). The shape of the immunoreactive somata varied as shown previously for GABAergic interneurons in the SC [13,25,27].

### 3.2. Distribution of GABA and GAD immunoreactivity in the deafferented SC

The laminar distribution pattern of immunolabeling for GABA and the two GADs in the deafferented SC was

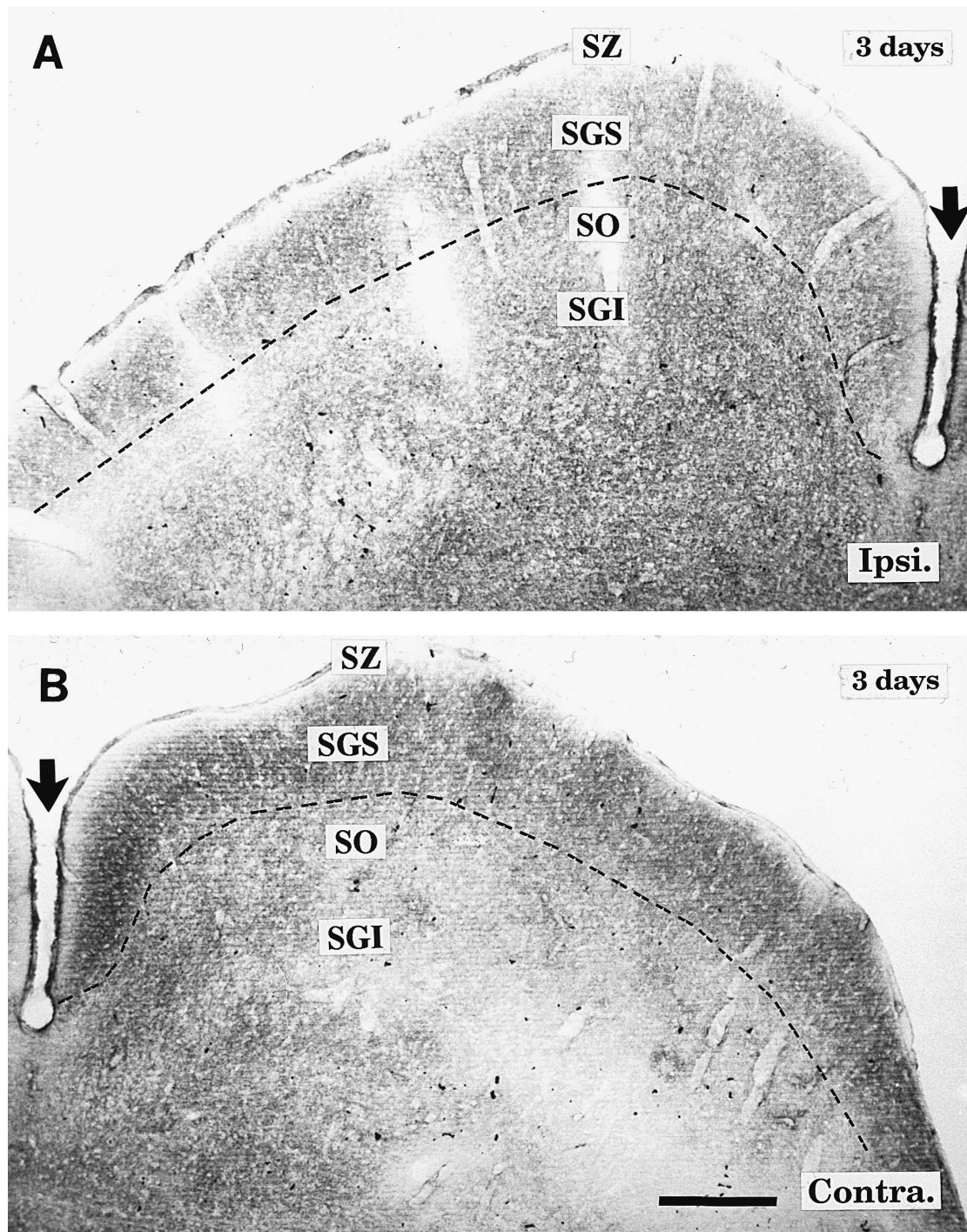


Fig. 3. Photomicrographs showing immunolabeling for GAT-1 in the ipsilateral (A) and contralateral (B) SC from a rat that survived for 3 days after unilateral optic nerve transection. Note the increased neuropil labeling in the SGS of the deafferented SC is present across its entire mediolateral extent (B) SZ: stratum zonale; SGS: stratum griseum superficiale; SO: stratum opticum. Broken lines indicate the lower border of the SGS. Arrow indicates midline. Scale bar = 200  $\mu$ m.

similar to that in the unaffected SC from operated animals (Fig. 1). Furthermore, the intensity of immunolabeling for these 3 markers did not show any differences between the two SC from these rats at the light microscopic level at all of the survival times examined in this study. However, the superficial layers of the SC contralateral to the lesion displayed a reduction in thickness that was evident at 7 days postlesion (Fig. 1A–C) and remained at later survival times (Fig. 1D–F). Therefore, the SC contralateral to the

optic nerve transection displayed a somewhat thinner band of immunolabeling for GABA and GADs.

### 3.3. Distribution of GAT immunoreactivity in the unaffected SC

#### 3.3.1. Light microscopy

Immunoreactivity for both GAT-1 and GAT-3 was found exclusively in the neuropil (Figs. 2–5). No somata

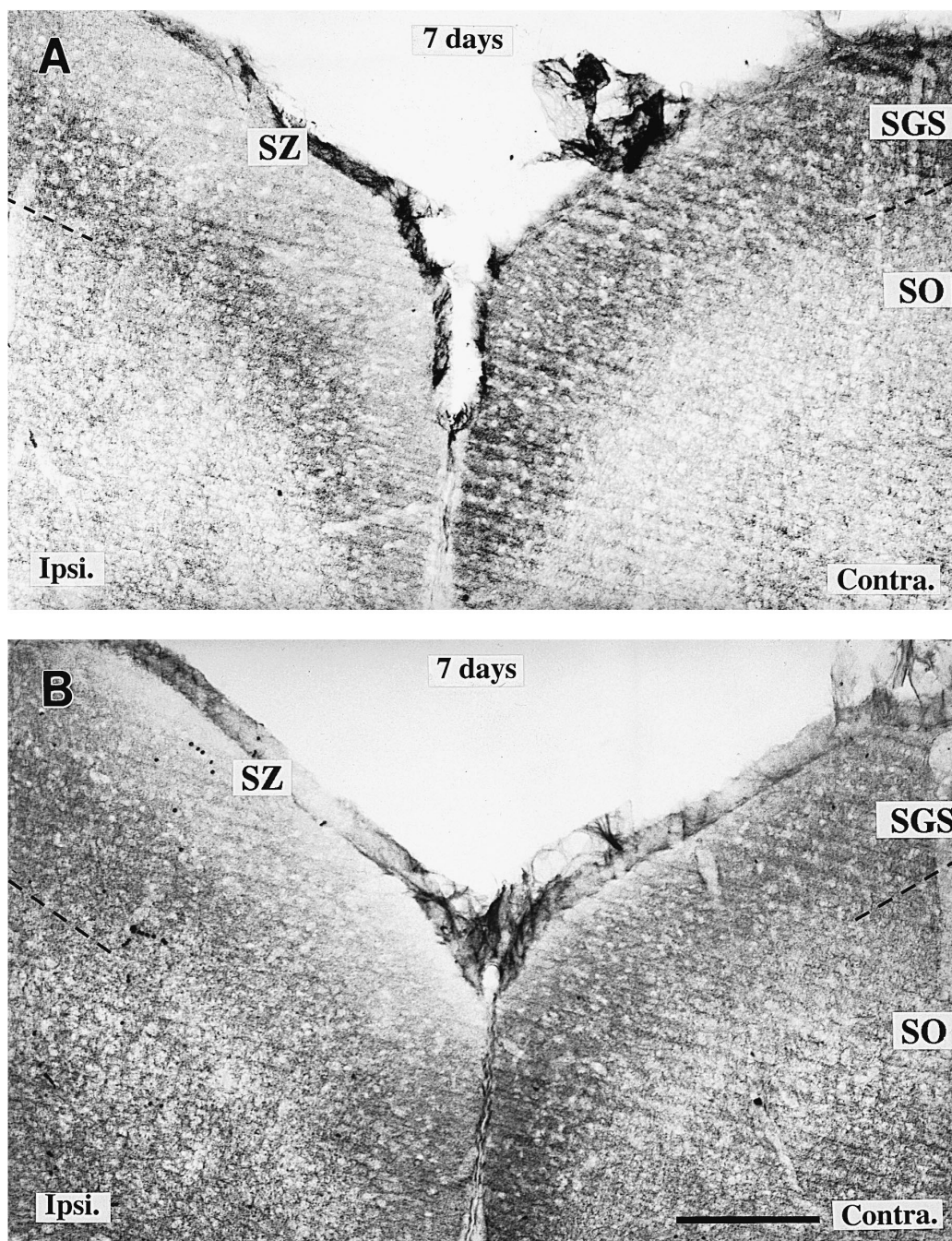


Fig. 4. Photomicrographs showing increased immunolabeling for GAT-1 (A) and GAT-3 (B) in the deafferented SC of rats, 7 days following nerve transection. Note that the superficial layers (SZ, SGS) of the SC are thinner in the contralateral (Contra.) side than the ipsilateral (Ipsi.) one, and the immunolabeling for both GATs are darker in the SGS of the denervated SC than its counterpart. Broken lines indicate the lower border of the SGS. SO: stratum opticum. Scale bar = 100  $\mu$ m.



were immunolabeled for either GAT-1 or GAT-3 at the light microscopic level. Light immunolabeling for GAT-1 and GAT-3 was present in the SZ, but dense immunostaining was found in the SGS. Immunoreactive puncta for GAT-1 and GAT-3 outlined unlabeled somata in the SGS (Figs. 4 and 5). The SO contained a light immunoreactivity for both GATs and it was organized in a reticular network. The non-visual layers deep to the SO displayed moderate

immunolabeling for GAT-1 and GAT-3 in the neuropil (Fig. 3A and Fig. 5).

### 3.3.2. Electron microscopy

At the electron microscopic level, GAT-1 immunoreactivity in the unaffected SC of operated rats was found in both neuronal and glial profiles (Fig. 6A–B). The neuronal profiles were mainly synaptic terminals that

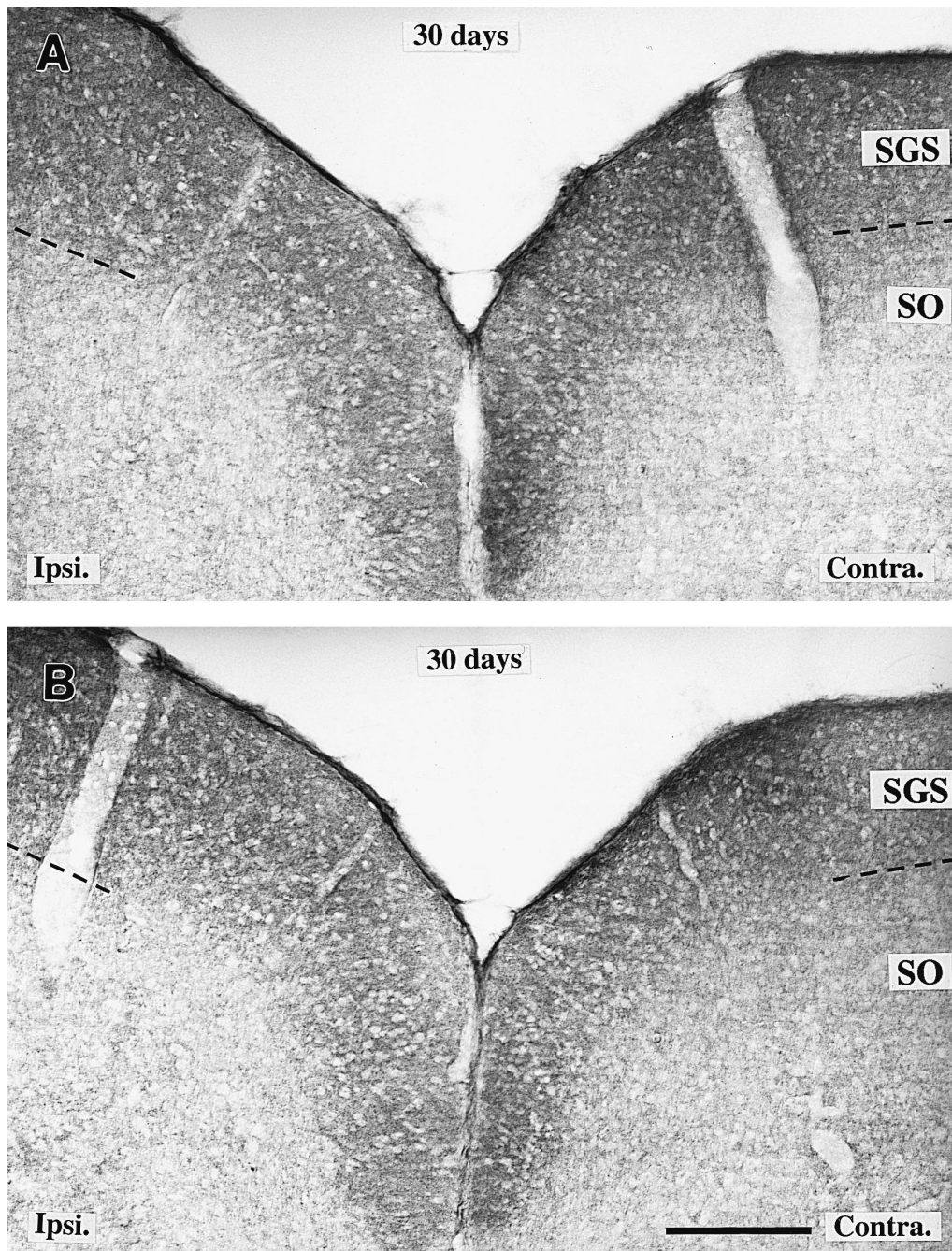


Fig. 5. Immunoreactivity for GAT-1 (A) and GAT-3 (B) in the rat SC, 30 days after unilateral optic nerve transection. The superficial layers of the contralateral (Contra.) SC are substantially reduced in thickness as compared to those of the ipsilateral (Ipsi.) SC. The neuropil labeling for both GATs is greater in the contralateral SC, but the difference in staining intensity is less pronounced than that in rats with a shorter survival time (cf., Fig. 2C–D, Fig. 3A–B and Fig. 4A–B). Broken lines indicate the lower border of the SGS. SO: stratum opticum. Scale bar = 100  $\mu$ m.

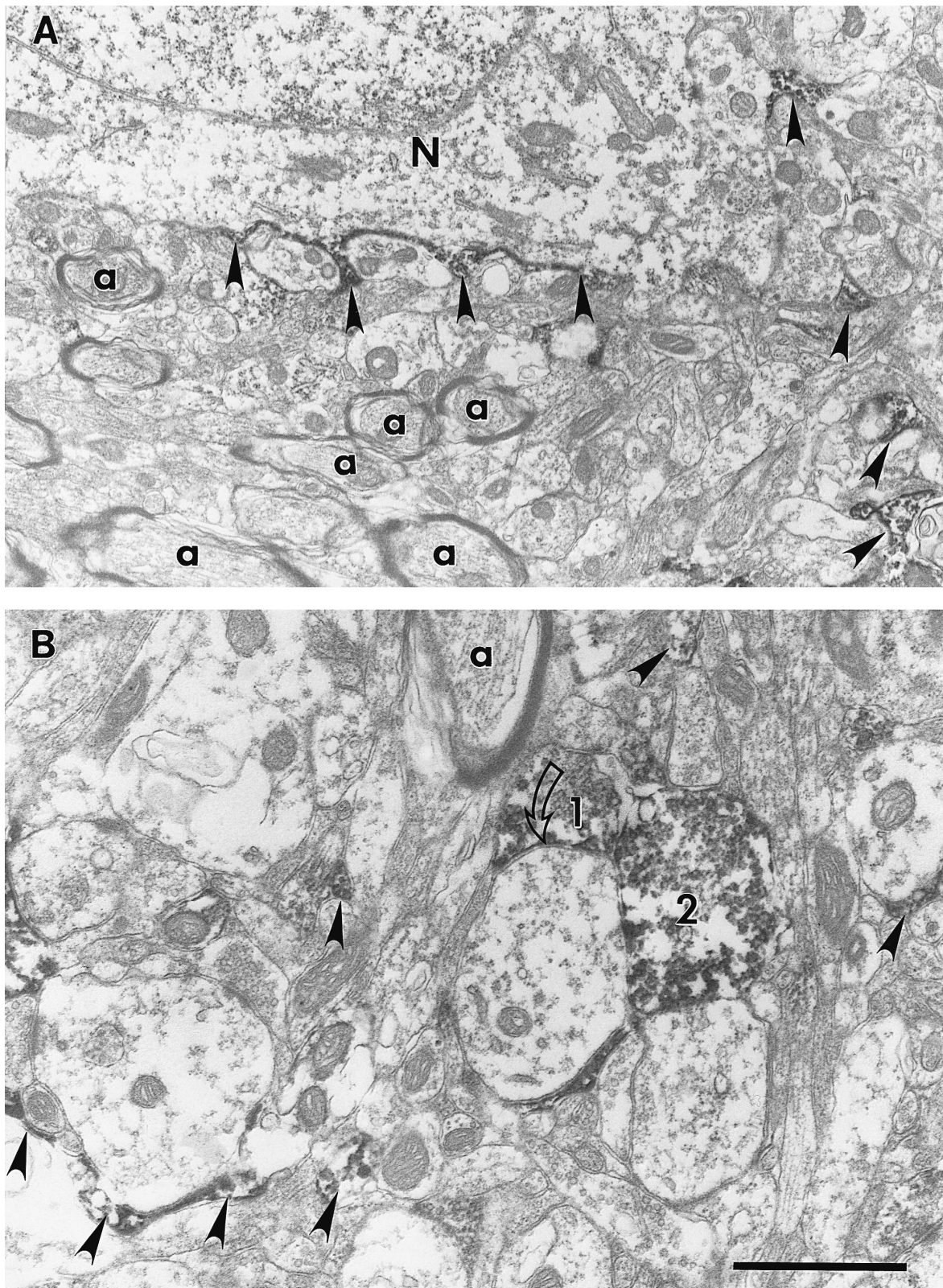


Fig. 6. Electron micrographs showing immunolabeling for GAT-1 in the SGS of an unaffected SC of a rat that survived for 7 days after an unilateral optic nerve transection. (A) shows labeled thin profiles of astrocytic processes (arrowheads) that appose an immunonegative neuronal somata (N) and are found in the neuropil. Many normal myelinated axons (a) are present. (B) shows GAT-1 immunoreactivity in two synaptic terminals (#1 and #2) and several astrocytic processes. The first terminal (#1) contains synaptic vesicles and forms a symmetric synapse (open arrow) with an immunonegative dendrite (D). The second (#2) also appears to have vesicles, but no synapses are associated with it. Note several labeled glial processes (arrowheads) scattered in the neuropil and apposed to pre- and postsynaptic structures. Scale bar = 1  $\mu$ m.

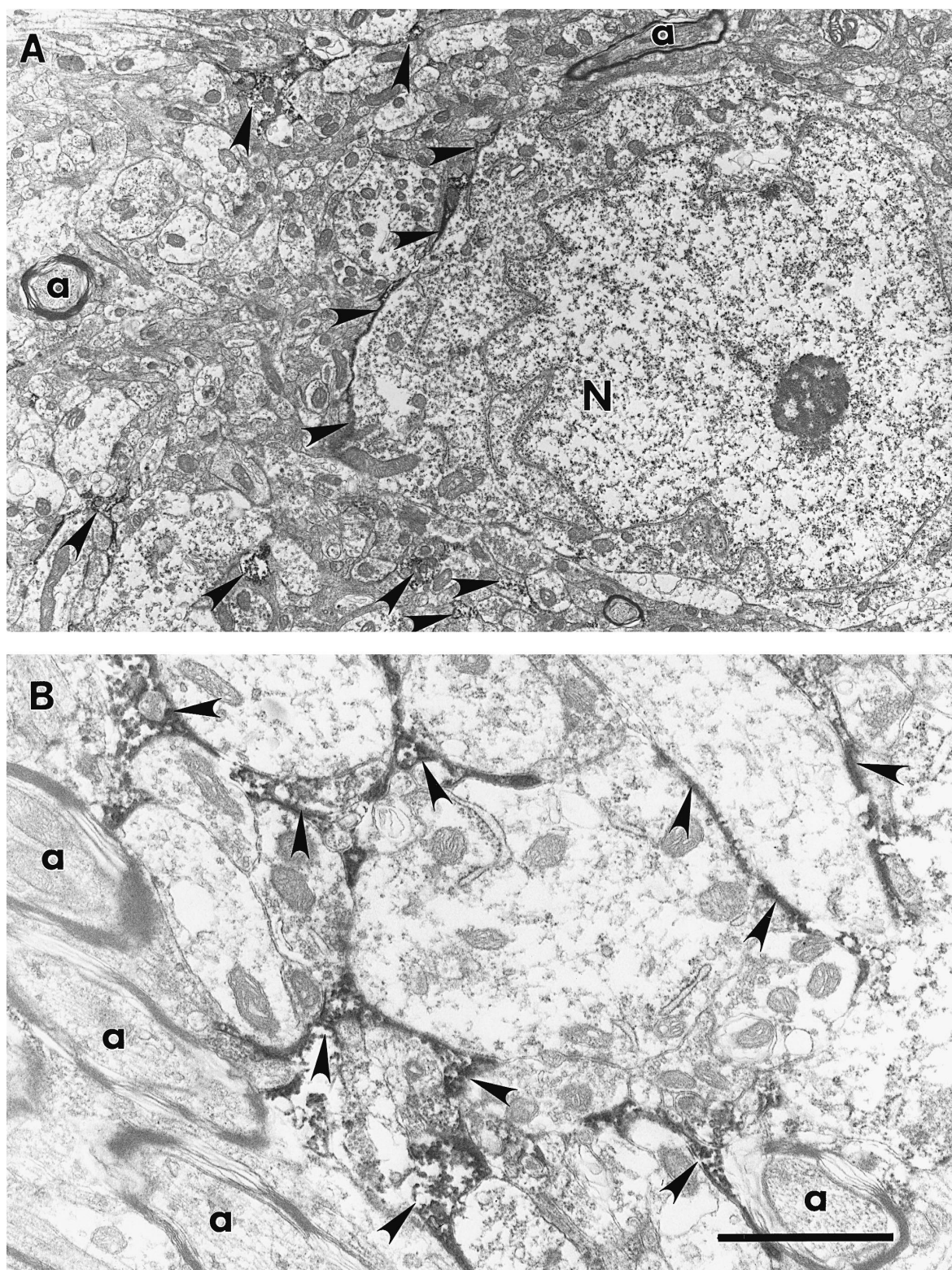


Fig. 7. Electron micrographs showing GAT-3 immunoreactivity in the SGS of an unaffected SC from a rat that survived for 7 days after unilateral optic nerve lesion. (A) shows labeled astrocytic processes (arrowheads) which appose an unlabeled soma (N) and extend between dendritic and axonal profiles. The labeled processes are small and thin, and are commonly apposed to pre- and postsynaptic structures. (B) shows GAT-3 immunolabeled astrocytic processes (arrowheads) in the neuropil that extend between dendrites and axon terminals. Several unlabeled synaptic terminals that are apposed by these labeled processes contain synaptic vesicles. Normal myelinated axons (a) are also shown. Scale bar = 4  $\mu$ m for (A) and 1  $\mu$ m for (B).



formed symmetric synapses with unlabeled somata and dendrites (Fig. 6B). No GAT-1 labeling was detected in the somata of SC neurons. The glial profiles with GAT-1

labeling were astrocytic processes and they were found to be more numerous than labeled synaptic terminals in any given area (Fig. 6). Most of the glial labeling appeared as

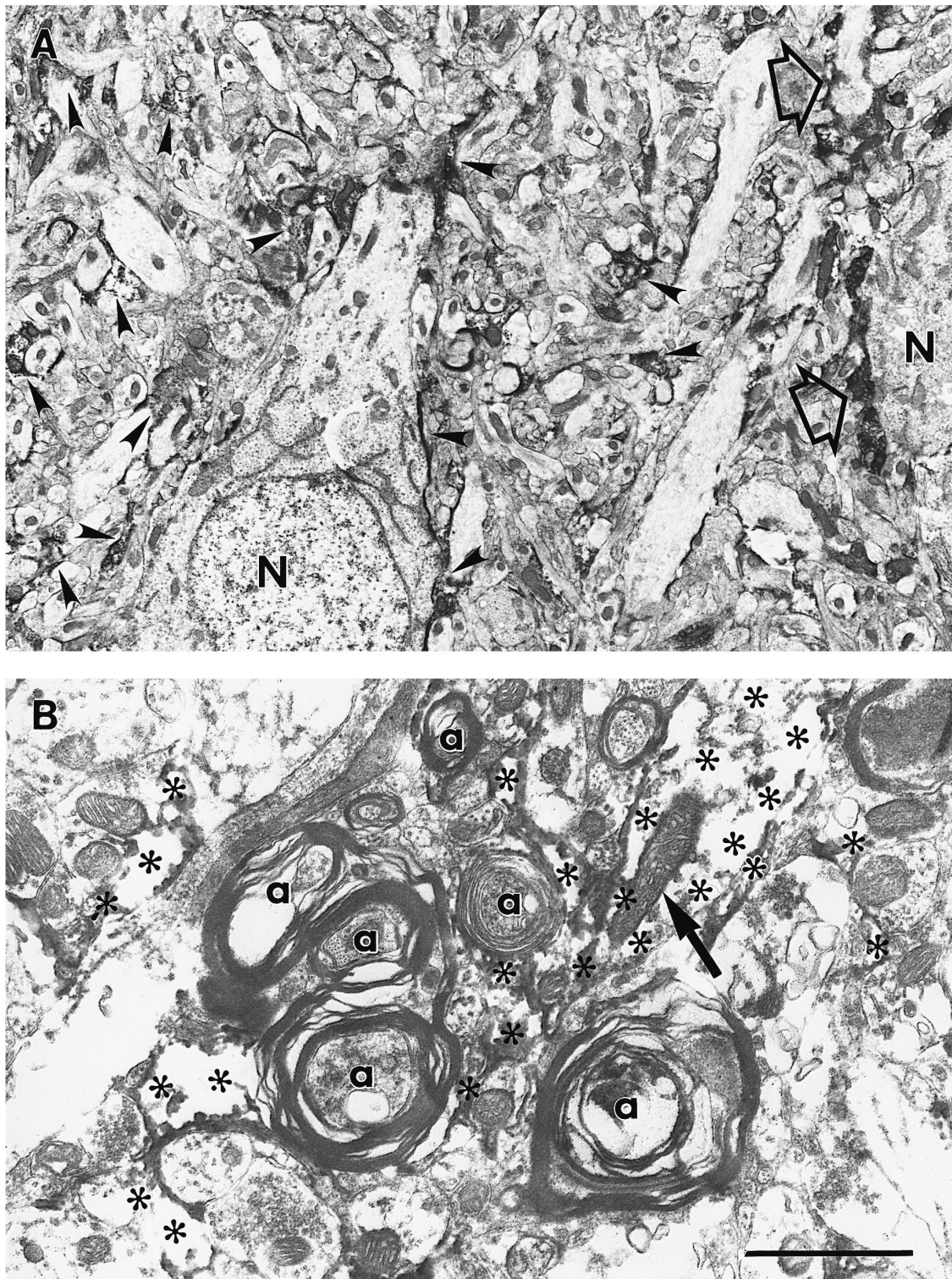


Fig. 8. Electron micrographs of GAT-1 immunoreactivity in the SGS of a deafferented SC, 7 days after optic nerve lesion. (A) shows numerous darkly labeled astrocytic processes (arrowheads) throughout the neuropil and adjacent to an unlabeled neuronal soma (N). Several large labeled profiles (open arrows) are swollen glial processes. (B) shows degenerating myelinated axons (a) and immunolabeled processes. The axons within the fibers are disorganized or disrupted. The myelin sheath of the fibers are separated, broken and collapsed. Immunolabeled swollen astrocytic processes (asterisks) are present between these degenerating axons, including one with a mitochondrion (solid arrow). Scale bar = 4  $\mu$ m for (A) and 1  $\mu$ m for (B).



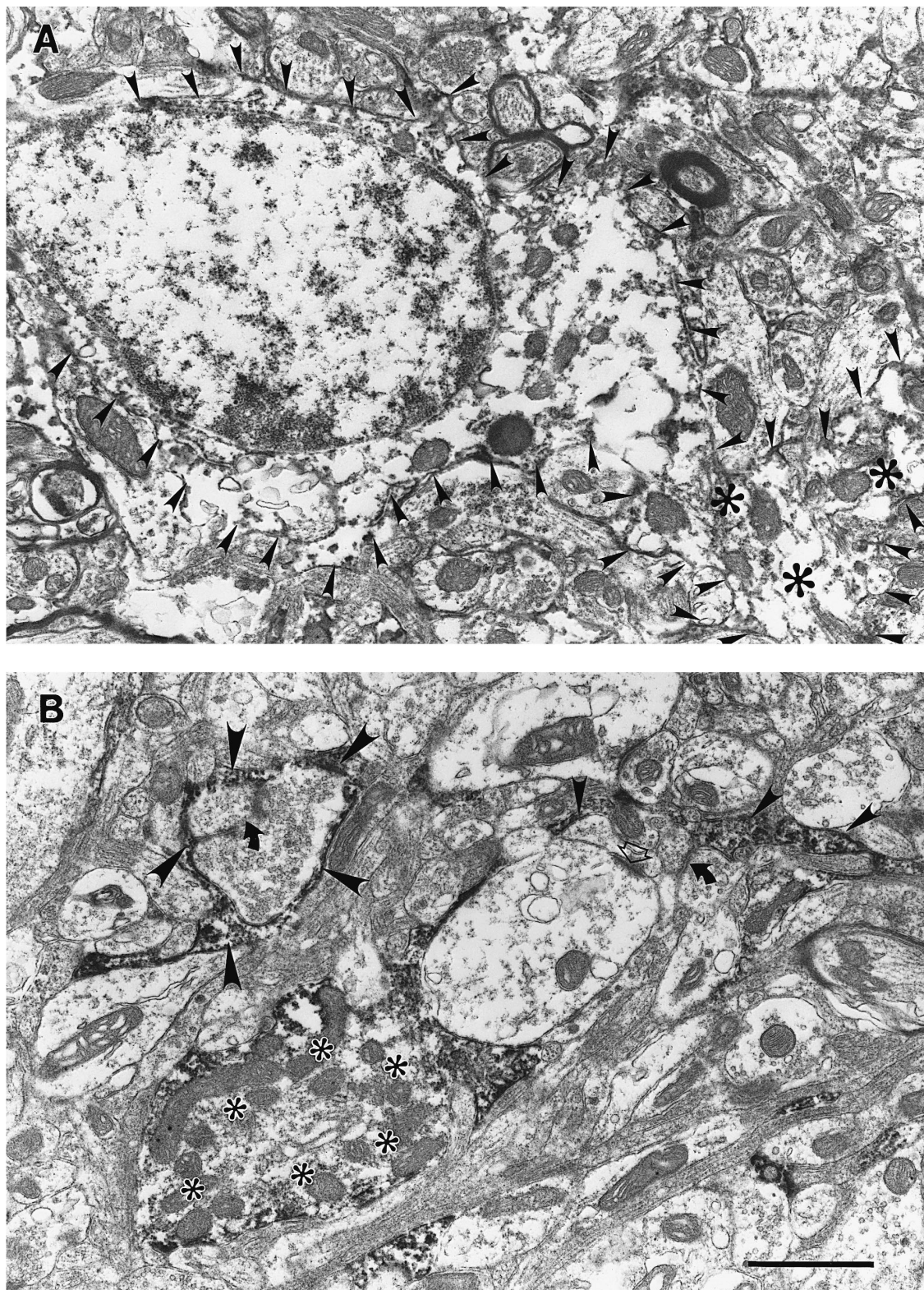


Fig. 9. Electron micrographs showing GAT-3 immunoreactivity in astrocytes in the SGS of the deafferented SC after a 7 day survival period. (A) shows a labeled astrocytic soma (outlined with arrowheads) with a wide shell of perikaryal cytoplasm. The immunolabeling is mainly present in the sublemmal regions. Some labeled processes (asterisks) of this cell extend into the neuropil. (B) shows labeled astrocytic processes, one of which is large and contains mitochondria. Again, the immunolabeling is concentrated in sublemmal regions of this process. The labeled astrocytic processes (arrowheads) in this area appose pre- and postsynaptic profiles of both symmetric (curved arrows) and asymmetric (open arrow) synapses. Scale bar = 1  $\mu$ m.

small individual profiles scattered in the neuropil (Fig. 6A–B). However, long, slender immunoreactive processes were also found and they were apposed to or extended along neuronal somata and dendritic shafts (Fig. 6A). The GAT-1 positive astrocytic processes in the neuropil often were associated or apposed to profiles that formed synapses. These synapses were both symmetric and asymmetric types (Fig. 6A–B). Immunoreactivity was also found within the glial endfoot processes on capillaries (not shown). GAT-1 immunolabeling of cell bodies of astrocytes was not observed.

The ultrastructural distribution of GAT-3 immunoreactivity in the unaffected SC was restricted to astrocytes, especially their processes (Fig. 7). Thin astrocytic profiles adjacent to neuronal somata displayed strong immunoreactivity for GAT-3 (Fig. 7A). In the neuropil, the immunolabeled astrocytic profiles were small in diameter, and many of them were elongated and associated with unlabeled dendritic profiles, including the proximal portion of primary dendrites. Other labeled glial processes were adjacent to synaptic terminals, and sometimes they surrounded both pre- and postsynaptic profiles (Fig. 7B).

### 3.4. Distribution of GAT immunoreactivity in the deafferented SC

#### 3.4.1. Light microscopy

The immunostaining for GAT-1 and GAT-3 exhibited substantial changes in the denervated SC at the light microscopic level. The immunolabeling for both GATs was increased slightly in the deafferented SC by the first day after the optic nerve lesion (Fig. 2A–B). This increase in immunostaining became greater at 3 days postlesion even though the thickness of the denervated SC was almost the same as that of the unaffected SC at this time (Fig. 2C–D). This change was present across the entire mediolateral extent of the SC (Fig. 3). In rats that survived 7 days, the increased immunoreactivity for GAT-1 and GAT-3 in the visual layers of the deafferented SC was remarkable (Figs. 4 and 5). Consistent with published data [41,46], the thickness of the visual layers of the deafferented SC was noticeably less than its counterpart (Fig. 4). The difference in immunolabeling for GAT-1 and GAT-3 between the two sides remained evident at 2–3 weeks after the lesion. Rats with 30 days postlesion survival displayed a heavier neuropil labeling for both GATs in the deafferented SC, though the degree of the difference in labeling intensity between the two sides was less pronounced as compared to those at earlier time points (cf., Fig. 2C–D, Figs. 4 and 5). The deafferentation-induced alteration in the immunostaining for GAT-1 and GAT-3 was not observed in the deeper layers of the deafferented SC (Figs. 4 and 5).

#### 3.4.2. Electron microscopy

The ultrastructural localization of GAT-1 and GAT-3 immunoreactivity in the visual layers of the deafferented

SC was obtained from operated animals that survived for 7 and 14 days. Preparations from these two time points showed similar electron microscopic findings. In these specimens, immunopositive astrocytes (Fig. 8A, Fig. 9) and immunonegative myelinated axons (Fig. 8B) displayed features that were different from those found in the unaffected SC, whereas the synaptic terminals labeled for GAT-1 were not found to be altered. Thus, the following description will focus on the former findings.

The frequency of labeled astrocytic processes for both GATs was much greater in the deafferented SC (Fig. 8A). The labeled processes in the denervated SC extended between dendritic and axonal processes in the neuropil and also surrounded neuronal somata (Fig. 8A). GAT-1 and GAT-3 immunolabeled processes were relatively larger in size and were more numerous as compared to those in the unaffected SC (cf., Figs. 6–9). Immunolabeling for GATs was detected in cell bodies that were identified as astrocytes based upon their size and their lack of synapses on their somata or processes (Fig. 9A). It is interesting to note that these labeled astrocytes from the deafferented SC contained more cytoplasm than their counterparts from the unaffected SC. The increase in the size of astrocytic somata and the number of processes immunolabeled for GATs indicated that astrocytes were hypertrophied. In both astrocytic somata or processes, immunolabeling for GAT-1 and GAT-3 was mainly present in the sublemmal region (Fig. 8B, Fig. 9A–B).

Ultrastructural changes for immunonegative profiles in the visual layers of the deafferented SC involved myelinated axons. These fibers showed apparent demyelination, and the axons within them were either disorganized or totally disappeared, indicating a terminal degeneration of retinal ganglion cell axons following optic nerve transection (Fig. 8B). GAT-1 or GAT-3 immunolabeled astrocytic processes were often seen between these degenerating fibers (Fig. 8B).

## 4. Discussion

The major finding of this experiment is that axotomy of the retinal ganglion cells induces an elevated immunostaining of two GABA transporters, GAT-1 and GAT-3, in astroglial cells in the deafferented SC. This change appears to be selective for the optic recipient layers of the SC. Our light and electron microscopic data indicate that the change in immunolabeling for both GATs is mainly a result of the reactive response of astrocytes and is not due to tissue shrinkage subsequent to retinal terminal degeneration. First, the increase in immunolabeling emerges as early as 1 day and is already substantial by 3 days after optic nerve lesion. At these time points, a reduction in the thickness of the visual layers in the deafferented SC is not evident [22,40,46]. Second, immunolabeling for GAT-1 to synaptic terminals was not altered in the deafferented SC at the examined time points. Further, there were no changes in

immunolabeling for two other GABAergic markers, GABA and GAD, in neuronal somata and puncta in the deafferented SC [26]. Thus, the enhanced labeling for GATs in the neuropil results from an increase of staining in astrocytes. Consistent with this conclusion are the electron microscopic data that show hypertrophied astrocytic processes and somata in the deafferented SC. It remains to be determined whether the glial hypertrophy is the only basis for the increased immunolabeling, or that an increased expression of GATs also occurs in astrocytes. In any event, these changes in the immunolabeling for GATs in the denervated SC would cause an increased uptake of GABA.

Other specific glial markers were shown to be upregulated in the denervated SC following optic nerve lesion or eye enucleation. They include the major histocompatibility complex (MHC) antigens in microglial cells [33] and glial fibrillary acidic protein (GFAP) in astrocytes [22,40]. It is interesting to note that an increase of GFAP expression appears within 1 day after optic nerve lesion in the affected SC [40] because at this same survival time the elevation of GATs first appeared. These findings indicate that terminal degeneration of retinal ganglion cell axons may induce the increase of both GFAP and GATs in astrocytes through similar mechanisms of neuron-glia intercommunication and interaction [22,41,42,44].

The finding of an increased staining of GATs in the deafferented SC is of considerable interest in that both pre- and postsynaptic markers of GABAergic synapses do not demonstrate remarkable changes in the deafferented SC in the first several weeks postlesion. For example, as shown in the present and previous studies the immunolabeling for GAD and GABA shows no changes in light microscopic distribution [13,26]. The binding activity for GABA-A receptor is also unchanged in the deafferented rat SC [5]. In addition, the overall GAD immunolabeled synaptic profiles in electron microscopic preparations are maintained in the deafferented SC, though a subtle change occurs in that the population of GAD-positive presynaptic terminals that form asymmetric synapses are increased. However, this latter change became evident only after 6 weeks postlesion and thus it was thought to be related to delayed neuroplastic responses of the tectal GABAergic neurons [13]. Therefore, the increase in GAT expression in astrocytes following deafferentation appears to be selective for this GABAergic synaptic parameter and suggests that GABA transporters are the most sensitive component of the GABAergic system to respond to optic nerve lesion.

#### 4.1. Functional considerations

There are no electrophysiological data available for the functional changes of GABAergic interneurons in the deafferented SC of the rat. However, Lyckman and Meyer [21] found that spontaneous tectal activity increased following optic deafferentation in goldfish. In contrast, it was interpreted that overall neuronal activity of the deafferented SC

in the rat was reduced as determined by glucose use [5,9]. Other data showed changes in some subtypes of glutamate receptors in this same experimental condition [6]. It is possible that functionally both excitatory and inhibitory neurons in the SC may alter their activity following deafferentation [5,6,9]. Elevated GAT-1 and GAT-3 levels in astrocytes may help to remove GABA more effectively after its release from axon terminals, and thus tone down inhibition in the deafferented SC. This affect would indicate a functional reorganization of GABAergic neurons following the loss of the retinal input that is known to be excitatory [25]. This notion is supported by the finding of activity-dependent transport of GABA in the brain [31]. Thus, the effect on GABA neurotransmission by its transporters in this experimental condition may serve as a mechanism to counterbalance the loss of excitatory drive to neurons within the deafferented optic recipient layers of the SC.

#### Acknowledgements

This study was supported by the National Science Foundation (IBN 9422392) and National Institute of Health (NS 15669). We thank Nicholas C. Brecha for providing GAT-1 and GAT-3 antibodies, Dr. Ronald L. Meyer for constructive comments, and Marian Shiba-Noz and Ellen Yi-Sing Lee for their excellent technical assistance.

#### References

- [1] D. Attwell, B. Barbour, M. Szatkowski, Nonvesicular release of neurotransmitter, *Neuron* 11 (1993) 401–407.
- [2] V.F. Balcar, I. Dammach, J.R. Wolff, Is there a non-synaptic component in the  $K^+$ -stimulated release of GABA in the developing rat cortex, *Dev. Brain Res.* 10 (1983) 309–311.
- [3] F.M. Benes, J. McSparren, E.D. Bird, S.L. Vincent, Deficits in small interneurons in prefrontal and cingulate cortices of schizophrenics and schizoaffective patients, *Arch. Gen. Psychiatry* 48 (1991) 996–1001.
- [4] L.A. Borden, K.E. Smith, T.A. Branchek, R.L. Weisshank, Molecular heterogeneity of the  $\gamma$ -aminobutyric acid (GABA) transport system, *J. Biol. Chem.* 267 (1992) 21098–21104.
- [5] D.T. Chalmers, J. McCulloch, Alterations in neurotransmitter receptors and glucose use after unilateral orbital enucleation, *Brain Res.* 540 (1991) 243–254.
- [6] D.T. Chalmers, J. McCulloch, Selective alterations in glutamate receptor subtypes after unilateral orbital enucleation, *Brain Res.* 540 (1991) 255–265.
- [7] E. Cherubini, J.L. Gaiarsa, Y. Ben-Ari, GABA: an excitatory transmitter in early postnatal life, *Trends Neurosci.* 14 (1991) 515–519.
- [8] J.A. Clark, A.Y. Deutch, P.Z. Gallipoli, S.G. Amara, Functional expression and CNS distribution of a  $\beta$ -alanine sensitive neuronal GABA transporter, *Neuron* 9 (1992) 337–348.
- [9] R.M. Cooper, G.A. Thurlow, Depression and recovery of metabolic activity in rat visual system after eye removal, *Exp. Neurol.* 89 (1985) 322–336.
- [10] M.J. During, K.M. Ryder, D.D. Spencer, Hippocampal GABA transporter function in temporal lobe epilepsy, *Nature* 376 (1995) 174–177.

- [11] M. Esclapez, N.J. Tillakaratne, D.L. Kaufman, A.J. Tobin, C.R. Houser, Comparative localization of two forms of glutamic acid decarboxylase and their mRNAs in rat brain supports the concept of functional differences between the forms, *J. Neurosci.* 14 (1994) 1834–1855.
- [12] J. Guastella, N. Brecha, H. Nelson, I. Czyzyx, S. Keynan, M.C. Miedel, N. Davidson, H.A. Lester, B.I. Kanner, Cloning and expression of a rat brain GABA transporter, *Science* 249 (1990) 1303–1306.
- [13] C.R. Houser, M. Lee, J.E. Vaughn, Immunocytochemical localization of glutamic acid decarboxylase in normal and deafferented superior colliculus: Evidence for reorganization of  $\gamma$ -aminobutyric acid synapses, *J. Neurosci.* 3 (1983) 2030–2042.
- [14] N. Ikegaki, N. Saito, M. Hashima, C. Tanaka, Production of specific antibodies against GABA transporter subtypes (GAT-1, GAT-2, GAT-3) and their application to immunocytochemistry, *Mol. Brain Res.* 26 (1994) 47–54.
- [15] L.L. Iversen, L.S. Kelly, Uptake and metabolism of  $\gamma$ -aminobutyric acid by neurons and glial cells, *Biochem. Pharmacol.* 24 (1975) 933–938.
- [16] J.M. Lauder, V.K.M. Han, P. Henderson, T. Verdoorn, A.C. Towle, Prenatal ontogeny of the GABAergic system in the rat brain: an immunocytochemical study, *Neuroscience* 19 (1986) 465–493.
- [17] G. Levi, M. Raiteri, Carrier-mediated release of neurotransmitters, *Trends Neurosci.* 16 (1993) 415–418.
- [18] F. Liang, E.G. Jones, Differential and time-dependent changes in gene expression for type II calcium/calmodulin-dependent protein kinase, 67 kDa glutamic acid decarboxylase, and glutamate receptor subunits in tetanus toxin-induced focal epilepsy, *J. Neurosci.* 17 (1997) 2168–2180.
- [19] Q.-R. Liu, B. Lopez-Carcuera, S. Mandiyan, H. Nelson, N. Nelson, Molecular characterization of four pharmacological distinct  $\gamma$ -aminobutyric acid transporters in the mouse brain, *J. Biol. Chem.* 268 (1993) 2106–2112.
- [20] R.D. Lund, Uncrossed visual pathways of the hooded and albino rats, *Science* 149 (1965) 1506–1507.
- [21] A.W. Lyckman, R.L. Meyer, Spontaneous and long-lived correlation in normal and denervated tectum of goldfish, *J. Neurobiol.* 26 (1995) 109–118.
- [22] S.C. McLoon, Response of astrocytes in the visual system to Wallerian degeneration: an immunohistochemical analysis of laminin and glial fibrillary acidic protein (GFAP), *Exp. Neurol.* 91 (1986) 613–621.
- [23] A. Minelli, N.C. Brecha, C. Karschin, S. DeBiasi, F. Conti, GAT-1, a high-affinity GABA plasma membrane transporter, is localized to neurons and astroglia in the cerebral cortex, *J. Neurosci.* 15 (1995) 7734–7748.
- [24] A. Minelli, S. DeBiasi, N.C. Brecha, L.V. Zuccarello, F. Conti, GAT-3, a high-affinity GABA plasma membrane transporter, is localized to astrocytic processes, and it is not confined to the vicinity of GABAergic synapses in the cerebral cortex, *J. Neurosci.* 16 (1996) 6255–6264.
- [25] R.R. Mize, G.D. Butler, Postembedding immunocytochemistry demonstrates directly that both retinal and cortical terminals in the cat superior colliculus are glutamate immunoreactive, *J. Comp. Neurol.* 371 (1996) 633–648.
- [26] R.R. Mize, Q. Luo, Visual deprivation fails to reduce calbindin 28K-D or GABA immunoreactivity in the rhesus monkey superior colliculus, *Vis. Neurosci.* 9 (1992) 157–168.
- [27] R.R. Mize, R.F. Spencer, P. Sterling, Two types of GABA-accumulating neurones in the superior gray layer of the cat superior colliculus, *J. Comp. Neurol.* 206 (1982) 180–192.
- [28] C.M. Müller, A role for glial cells in activity-dependent central nervous plasticity? Review and hypothesis, *Int. Rev. Neurobiol.* 34 (1992) 215–281.
- [29] R.W. Olsen, M. Avoli, GABA and epileptogenesis, *Epilepsia* 38 (1997) 399–407.
- [30] R. Pinord, J. Benfares, L. Lanoir, Electron microscopic study of GABA-immunoreactive neuronal processes in the superficial gray layer of the rat superior colliculus: Their relationship with degenerating retinal nerve endings, *J. Neurocytol.* 20 (1991) 262–276.
- [31] D.V. Pow, W. Baldrige, D.K. Crook, Activity-dependent transport of GABA analogues into specific cell types demonstrated at high resolution using a novel immunocytochemical strategy, *Neuroscience* 73 (1996) 1129–1143.
- [32] R. Radian, O.P. Ottersen, J. Storm-Mathisen, M. Castel, B.I. Kanner, Immunocytochemical localization of the GABA transporter in rat brain, *J. Neurosci.* 10 (1990) 1319–1330.
- [33] K. Rao, R.D. Lund, Optic nerve degeneration induces the expression of MHC antigens in the rat visual system, *J. Comp. Neurol.* 336 (1993) 613–627.
- [34] M. Rattray, J.V. Priestley, Differential expression of GABA transporter-1 messenger RNA in subpopulations of GABA neurons, *Neurosci. Lett.* 156 (1993) 163–166.
- [35] G.P. Reynolds, C. Czudek, H.B. Andrews, Deficit and hemispheric asymmetry of GABA uptake sites in the hippocampus in schizophrenia, *Biol. Psychiatry* 27 (1990) 1038–1044.
- [36] C.E. Ribak, Local circuitry of GABAergic basket cells in the dentate gyrus, *Epilepsy Res.* 7 (Suppl) (1992) 29–47.
- [37] C.E. Ribak, A.B. Harris, J.E. Vaughn, E. Roberts, Inhibitory, GABAergic nerve terminals decrease at sites of focal epilepsy, *Science* 205 (1979) 211–214.
- [38] C.E. Ribak, W.M.Y. Tong, N.C. Brecha, The GABA plasma membrane transporters, GAT-1 and GAT-3, display different distributions in the rat hippocampus, *J. Comp. Neurol.* 367 (1996) 595–606.
- [39] C.E. Ribak, W.M.Y. Tong, N.C. Brecha, Astrocytic processes compensate for the apparent lack of GABA transporters in the axon terminals of cerebellar Purkinje cells, *Anat. Embryol.* 194 (1996) 379–390.
- [40] R. Schmidt-Kastner, D. Meller, U.T. Eysel, Immunohistochemical staining for glial fibrillary acidic protein (GFAP) after deafferentation or ischemic infarction in the rat visual system: Features of reactive and damaged astrocytes, *Int. J. Neurosci.* 11 (1992) 157–174.
- [41] F. Schon, J.S. Kelly, Selective uptake of  $[H^3]\beta$ -alanine by glia: association with the glial uptake system for GABA, *Brain Res.* 86 (1975) 243–257.
- [42] A. Schousboe, N. Westergaard, K. Sonnewald, S.B. Peterson, A.C.H. Yu, L. Hertz, Regulatory role of astrocytes for neuronal biosynthesis and homeostasis of glutamate and GABA, *Prog. Brain Res.* 94 (1992) 199–211.
- [43] M. Swan, A. Najlerahim, R.E.B. Watson, J.P. Bennett, Distribution of mRNA for the GABA transporter GAT-1 in the rat brain: evidence that GABA uptake is not limited to presynaptic neurons, *J. Anat.* 185 (1994) 315–323.
- [44] A. Vernadakis, Glia-neuron intercommunications and synaptic plasticity, *Prog. Neurobiol.* 49 (1996) 185–214.
- [45] X.X. Yan, W.A. Cariaga, C.E. Ribak, Immunoreactivity for GABA plasma membrane transporter, GAT-1, in the developing rat cerebral cortex: transient presence in the somata of neocortical and hippocampal interneurons, *Dev. Brain Res.* 99 (1997) 1–19.
- [46] X.X. Yan, L.J. Garey, Y. Liang, K.A. von Bussmann, L.S. Jen, Increased expression of NADPH-diaphorase in visual centers after unilateral optic nerve transection in the rat, *J. Brain Res.* 36 (1995) 485–488.
- [47] X.X. Yan, L.S. Jen, L.J. Garey, NADPH-diaphorase-positive neurons in the primate cerebral cortex colocalize with GABA and calcium binding proteins, *Cerebral Cortex* 6 (1996) 524–529.
- [48] X.X. Yan, C.E. Ribak, Increased expression of GABA transporters, GAT-1 and GAT-3, in the superior colliculus following optic nerve transection, *Soc. Neurosci. Abstr.* 23 (1997) 7955.
- [49] X.X. Yan, D.S. Zheng, L.J. Garey, Prenatal development of GABA immunoreactive neurons in the human striate cortex, *Dev. Brain Res.* 65 (1992) 191–204.